Catal Lett (2008) 121:131–136
DOI 10.1007/s10562-007-9309-0

Photocatalytic Study of Bi-ZSM-5 and Bi_2O_3/HZSM-5 for the Treatment of Phenolic Wastes

Jakkidi Krishna Reddy · Kannekanti Lalitha · Valluri Durga Kumari · Machiraju Subrahmanyam

Received: 20 August 2007 / Accepted: 9 October 2007 / Published online: 30 October 2007

Abstract Bi-ZSM-5 and Bi_2O_3/HZSM-5 with varying amounts of (1, 3, and 5 wt.%) of Bi_2O_3 were prepared by impregnation and solid state dispersion (SSD) methods. These catalysts were characterized by XRD, UV–Vis DRS, XPS, and BET surface area techniques. Characterization of these catalysts by DRS clearly shows a blue shift of >100 nm in the absorption band edge of Bi_2O_3 (band gap shift from 2.75 to 3.5 eV) in the samples prepared by impregnation and a blue shift of 50 nm in the samples prepared by SSD methods indicating that Bi_2O_3 is in interaction with the support in impregnated samples. XPS studies are also in favor of this observation. The photocatalytic activities of these systems were evaluated in the degradation of phenol under UV irradiation. Catalysts prepared by impregnation method are showing good photocatalytic activity compared to catalysts prepared by SSD method. Based on the characterization and photodegradation activity of the Bi-ZSM-5 catalysts a structure–activity correlation has been established for the effective treatment of phenolic wastes.

Keywords Bi-ZSM-5 · Bi_2O_3/HZSM-5 · Novel photocatalyst · Phenol degradation

1 Introduction

Heterogeneous semiconductor photocatalysis has gained a lot of importance in the recent years, because it is used to decompose the organic pollutants present in the industrial wastes. Photocatalytic treatment of environmental pollutants using semiconductors like TiO_2, Cds, Fe_2O_3, etc., is well reported [1–7]. When semiconductors are illuminated with light greater or equal to their band gap energy, generate electrons and holes that decompose organic molecules into carbon dioxide and water. The major problem with the semiconductor photocatalysts is the faster electron–hole recombination observed in nanoseconds that decreases the charge transfer efficiency from the surface of the photocatalyst to the substrate molecule, which results in the decreased photoefficiency of the catalyst system. In order to reduce the rate of electron–hole recombination and to modify the properties of the photocatalysts several methods have been employed, like selective doping of photocatalyst with metals [8] and dispersion of photocatalysts over zeolite supports [9, 10]. Zeolites with adsorption properties pool the organic pollutants to the vicinity of the dispersed photocatalyst and decrease the electron–hole recombination by accepting the electrons (Lewis acid) from the surface of the catalyst enhancing the photocatalytic activity. Another important advantage of dispersing photocatalyst over zeolites is to increase the band gap energy. When a semiconductor oxide is loaded in small amounts on the zeolites, exists as nanosized particle in a highly dispersed form with increased band gap energy and decreased rate of electron–hole recombination that increases photoactivity of the catalyst [11–13]. So far investigations on photocatalytic activity of titania are well acknowledged by modifying its properties for the photooxidation of organic pollutants.

However the present trend is to modify and explore other semiconductor oxides that can be used as photocatalysts. For example Bi_2O_3, a semiconductor with a wide band gap ranging from 2 to 3.9 eV [14–17] was used as a

J. K. Reddy · K. Lalitha · V. Durga Kumari (✉) · M. Subrahmanyam
Inorganic and Physical Chemistry Division, Indian Institute of Chemical Technology, Hyderabad 500 007, India
e-mail: durgakumari@iict.res.in

photocatalyst in photodegradations [18, 19]. Earlier reports also proved *bismuth based* oxychlorides with modified band gaps as efficient photocatalysts for the degradation of organic pollutants [20, 21]. It is known that Bi_2O_3 exhibits polymorphism that exists in six forms α', β, γ, δ, ε', and ω [22, 23]. Among them the low temperature α' and high temperature δ are the stable phases and other forms are the high temperature meta stable phases and every phase is associated with certain band gap energy [16]. It was also studied that bismuth oxide films calcined at 550 °C are composed of more tetragonal phase (β) with maximum electron binding energy and high band gap showing good *photocatalytic* activity [18, 19]. The present investigation is an attempt to study the photocatalytic activity of interacted and dispersed bismuth oxide supported over HZSM-5 zeolite in phenol degradation under UV irradiation.

2 Experimental

2.1 Chemicals

HZSM-5 with Si/Al_2 = 27.5 and 250 are from PQ Corporation (Netherlands). $Bi(NO_3)_3 \cdot 5H_2O$ and Bi_2O_3 are from Loba Chemie, GR grade (India). HNO_3 and HPLC grade methanol were from Rankem (India).

2.2 Preparation of Bi-ZSM-5 Catalysts (Impregnation)

Bi-ZSM-5 catalysts were prepared by the impregnation of required amount (for 1, 3, and 5 wt.% of Bi_2O_3) of $Bi(NO_3)_3 \cdot 5H_2O$ salt dissolved in minimum quantity of dil. HNO_3 added to HZSM-5. The mixture was dried slowly on a hot plate initially and then in an oven at 100 °C over night followed by calcination at 550 °C for 5 h.

2.3 Preparation of Bi_2O_3/HZSM-5 Catalysts (SSD)

Bi_2O_3/HZSM-5 catalysts were prepared by mixing required amount (for 1, 3, and 5 wt.%) of Bi_2O_3 with HZSM-5 using alcohol for thorough mixing in mortar pestle and the dried samples obtained in this course were allowed for further drying in the oven at 100 °C and calcined finally at 550 °C for 4 h.

2.4 Catalyst Characterization

Powder XRD patterns were recorded with a Siemens D-5000 X-ray diffractometer using CuKα radiation. UV–Vis DR spectra were recorded on Cintra 10_e spectrometer using pellets of 50 mg sample ground with 2.5 g of KBr. XPS were recorded on a KRATOS AXIS 165 photoelectron spectroscopy using the MgKα radiation (150 W) anode, taking C 1s level as internal standard. BET surface area of HZSM-5 and Bi loaded HZSM-5 samples were measured in all glass high vacuum by N_2 adsorption at –196 °C.

2.5 Photocatalytic Experiments

In a typical photocatalytic experiment phenol solution of 40 mL (10^{-4} M) was taken in a quartz reactor and 120 mg of catalyst was added (3 g L^{-1}). 250 W mercury vapor lamp was used as UV source. Prior to start of light experiments dark adsorption experiments were carried out for 1 h under continuous stirring. Samples taken at regular intervals were filtered through 0.2 µm bore filters and analyzed by HPLC using C-18 Phenomenex (5 µm), 250×4 mm^2 column and methanol/water (1:1) mobile phase at λ_{max} 220 nm.

3 Results and Discussion

3.1 BET Surface Area

The surface area of the parent zeolite HZSM-5 (395 m^2 g^{-1}) decreased in general on supporting Bi_2O_3. As can be seen from Table 1 the decrease in surface area is more for the catalysts prepared by SSD compared with the catalysts prepared by impregnation method and it must be noted that acidification of the impregnating solutions with HNO_3 produces the catalysts with slightly lower surface area [24].

3.2 XRD

Powder X-ray diffractograms of Bi-ZSM-5 samples are shown in Fig. 1. It can be seen from the spectra that Bi_2O_3 calcined at 550 °C is composed of monoclinic and tetragonal phases and the high intense peaks of tetragonal phase confirm

Table 1 Physical characterization of Bi modified HZSM-5 catalysts

S.No.	Catalysts	Surface area (m^2 g^{-1})
1.	HZSM-5	395
2.	1 wt.% Bi-ZSM-5 (Imp)	242
3.	3 wt.% Bi-ZSM-5 (Imp)	225
4.	5 wt.% Bi-ZSM-5 (Imp)	204
5.	1 wt.% Bi_2O_3/HZSM-5 (SSD)	230
6.	3 wt.% Bi_2O_3/HZSM-5 (SSD)	200
7.	5 wt.% Bi_2O_3/HZSM-5 (SSD)	186

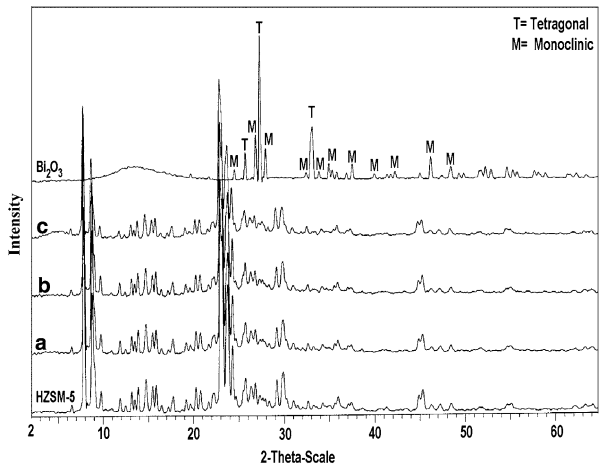

Fig. 1 XRD patterns of HZSM-5, Bi-ZSM-5, and Bi_2O_3: (**a**) 1, (**b**) 3, and (**c**) 5 wt.% Bi_2O_3

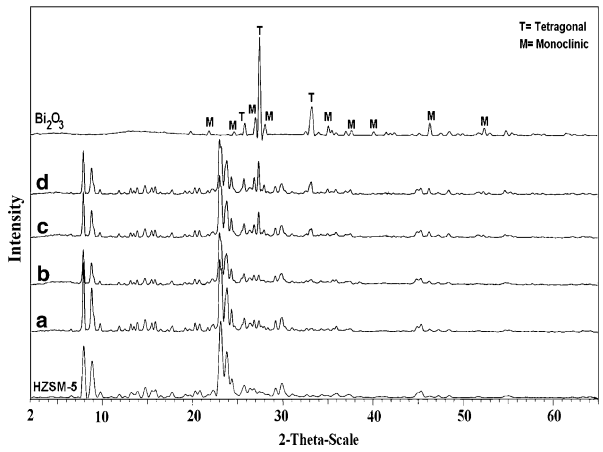

Fig. 2 XRD patterns of HZSM-5, Bi_2O_3/HZSM-5, and Bi_2O_3: (**a**) 1, (**b**) 3, (**c**) 5, and (**d**) 10 wt.%

the presence of this phase in major amount compared to the monoclinic phase [18, 19]. On impregnating bismuth over the zeolite, no characteristic peaks of crystalline Bi_2O_3 phase are observed even at high loadings (5 wt.%) of Bi_2O_3. This suggests that the dispersed Bi_2O_3 species over HZSM-5 are nanosized particles that escape the XRD detection. In the XRD patterns of Bi_2O_3/HZSM-5 (SSD) samples (Fig. 2), tetragonal and monoclinic phases are clearly observed at 5 wt.% Bi_2O_3 loading on HZSM-5 indicating that Bi_2O_3 particles are relatively bigger in size compared to the particles in impregnated samples. The size variation of these particles is also supported by our DRS results.

3.3 UV–Vis DRS

UV–Vis DRS of Bi_2O_3, Bi-ZSM-5, and Bi_2O_3/HZSM-5 measured are shown in Figs. 3 and 4. These spectra are

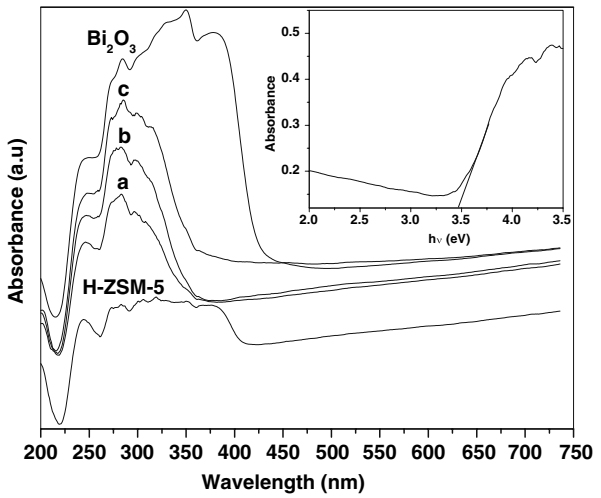

Fig. 3 UV–Vis DRS of HZSM-5, Bi-ZSM-5, and Bi_2O_3: (**a**) 1, (**b**) 3, and (**c**) 5 wt.% Bi_2O_3. Inset figure is a plot of absorbance vs. photon energy ($h\nu$) in eV for 3 wt.% Bi-ZSM-5

examined to understand the size quantization effect, band gap, and the Bi_2O_3 interaction with the zeolite support. The bulk Bi_2O_3 semiconductor showed a large absorption band around 450 nm resulted by the electron transition from oxygen valence band to the bismuth conduction band that corresponds to the band gap energy of 2.75 eV, calculated by the formula $\lambda_g = 1{,}239.8/E_g$ [20]. In bismuth impregnated zeolite at low loadings the absorption band is blue shifted by about 100 nm that resulted in the increased band gap and the shift is decreased with increasing Bi_2O_3 loading. This large blue shift in the absorption band edge may be seen as due to the interaction of isolated bismuth particles with the support. Earlier reports on low wt.% of Ti with MCM-41 established a blue shift >100 nm as a result of interaction with the support [25]. In the case of SSD samples a blue shift of <50 nm in the absorption edge

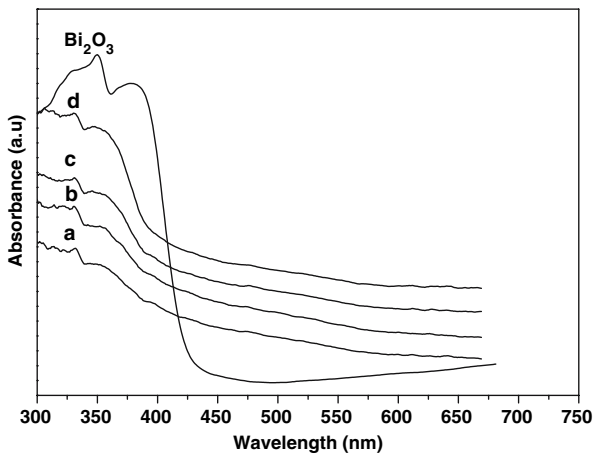

Fig. 4 UV–Vis DRS of Bi_2O_3/HZSM-5 and Bi_2O_3: (**a**) 1, (**b**) 3, (**c**) 5, and (**d**) 10 wt.%

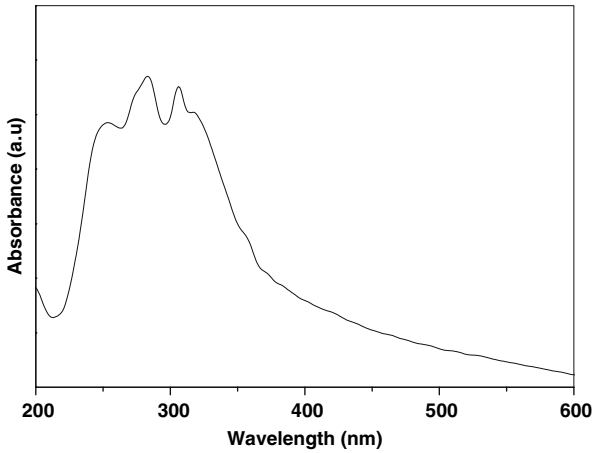

Fig. 5 UV–Vis DRS of Bi-ZSM-5 (3 wt.% Bi_2O_3, Si/Al_2 = 250)

indicates the size quantization of Bi_2O_3 particles and this is decreased with an increase in Bi_2O_3 loading. Band gap variation with respect to size of the particles is in agreement with the earlier reports [14]. The band gap energy (*Eg* value) of 3 wt.% Bi-ZSM-5 is estimated from a plot of absorbance versus photon energy (*hv*). The absorbance is extrapolated to get the band energy for the Bi-ZSM-5 photocatalyst with good approximation [20] as shown in Fig. 3 (inset). The estimated band gap energy of the sample is around 3.5 eV. To know the effect of Si/Al_2 ratio of the zeolite on the extent of bismuth interaction, UV–Vis DRS of 3 wt.% Bi-ZSM-5 with Si/Al_2 = 250 is recorded. It is clear from the Fig. 5 that 3 wt.% Bi-ZSM-5 (Si/Al_2 = 250) with neglizable Al content is showing a blue shift of 50 nm, which is less compared to that of 3 wt.% Bi-ZSM-5 (Si/Al_2 = 27.5). These studies show that the presence of Al that give rise to Bronsted acidic sites are essential for Bi to establish linkages with the zeolite support. Thus DRS studies clearly show that chemical environment of Bi in samples prepared by impregnation method is different from the samples prepared by SSD method.

3.4 XPS

In order to elucidate further the chemical environment of Bi that is in interaction with support HZSM-5, the impregnated catalysts are subjected to XPS measurements and the spectra are shown in Fig. 6. In 1 and 3 wt.% Bi impregnated samples the Bi $4f_{7/2}$ and Bi $4f_{5/2}$ binding energies are slightly more compared to the values of bismuth in pure Bi_2O_3 [26, 27] as shown in Table 2. This variation may be seen as due to the decrease of electron density around bismuth resulting by the interaction of the Bi with the support. The small variation in Bi $4f_{7/2}$ and Bi $4f_{5/2}$ binding energies

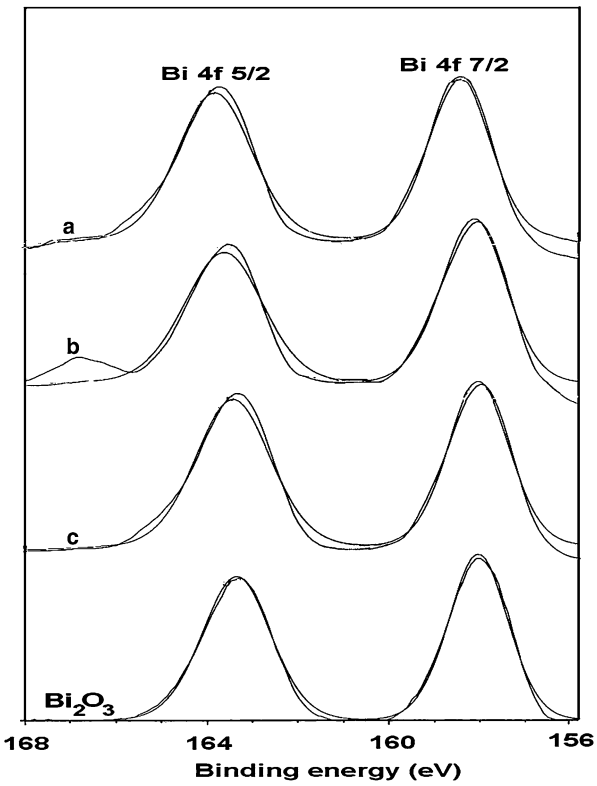

Fig. 6 XPS of Bi-ZSM-5 and Bi_2O_3: (**a**) 1, (**b**) 3, and (**c**) 5 wt.% Bi_2O_3

do not support change in the oxidation state of bismuth. At 5 wt.% Bi loading the change in the Bi $4f_{7/2}$ and Bi $4f_{5/2}$ values are negligible representing that the particles are not in interaction with the support. To understand the chemical environment of Bi in SSD samples, XPS measurements were also performed for 3 wt.% Bi_2O_3/HZSM-5 catalyst (Fig. 7), no remarkable change is observed in the binding energies of Bi $4f_{7/2}$ and Bi $4f_{5/2}$. From the XPS results it is clearly understood that in SSD samples Bi_2O_3 is simply dispersed *without* any interaction with the support, where as in impregnated samples Bi_2O_3 is highly dispersed and is in interaction with the support.

Table 2 Binding energy values of Bi modified HZSM-5 catalysts

S.No	Catalysts	Binding energy values (eV)	
		$4f_{5/2}$	$4f_{7/2}$
1.	1 wt.% Bi-ZSM-5 (Imp)	163.868	158.498
2.	3 wt.% Bi-ZSM-5 (Imp)	163.750	158.356
3.	5 wt.% Bi-ZSM-5 (Imp)	163.401	158.053
4.	3 wt.% Bi_2O_3/HZSM-5 (SSD)	163.396	158.048
5.	Bi_2O_3	163.397	158.047

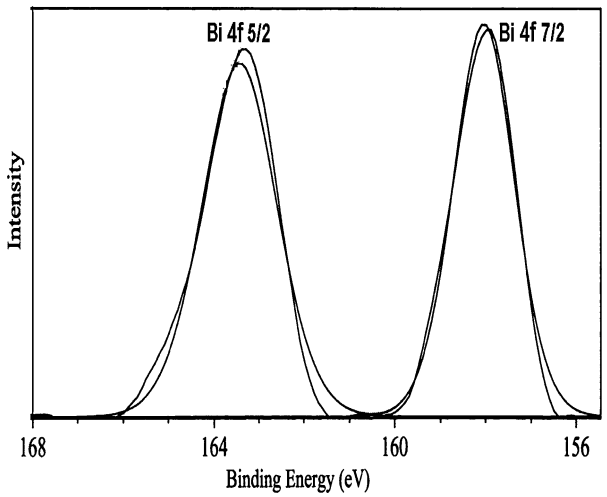

Fig. 7 XPS of 3 wt.% Bi_2O_3/H-ZSM-5 catalysts

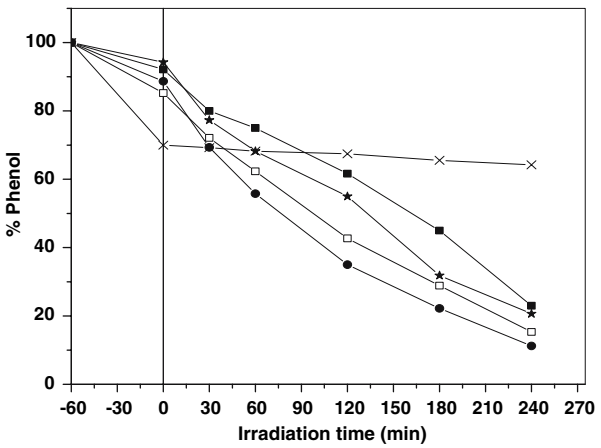

Fig. 9 Photocatalytic degradation of phenol (10^{-4} M) over (×) HZSM-5 and Bi_2O_3/HZSM-5: (□) 1 wt.%, (●) 3 wt.%, (★) 5 wt.%, and (■) 10 wt.%

3.5 Photocatalytic Activity

The photocatalytic activity of Bi-ZSM-5 and Bi_2O_3/HZSM-5 in the degradation of phenol under UV irradiation is shown in Figs. 8 and 9. Photolysis experiments show about 7% phenol degradation. Dark experiments show 30% phenol adsorption on bare HZSM-5. Bi_2O_3 loading generally decreases the adsorption of phenol independent of the method of catalyst preparation, however, impregnated samples with high surface area show maximum adsorption (about 20%) of phenol as compared to SSD samples. Among the impregnated Bi-ZSM-5 catalysts highest photodegradation activity is seen on 3 wt.% Bi-ZSM-5 and complete mineralization of phenol is observed with in 2 h on this particular photocatalyst. The enhanced photocatalytic activity of Bi-ZSM-5 catalysts may be seen as due to (1) adsorption properties of HZSM-5 that pool the phenol molecules in vicinity of the photocatalyst resulting in synergistic activity, (2) zeolite with acidic properties (Lewis acid) acts as electron scavenger, which increases the hole concentration making the degradation faster, and (3) Bi_2O_3 particles in highly dispersed and interacted are nano-sized with an increased band gap of 2.75 to 3.5 eV that decreases the rate of electron–hole recombination facilitating charge transfer from the surface of the catalyst to the substrate molecule. The interaction and increased band gap of the catalyst Bi-ZSM-5, evidenced by XPS and UV–Vis DRS techniques are in favor of these observations. This is also further supported by studying the effect of Si/Al_2 ratio of zeolite on the photoactivity of the catalyst. Thus 3 wt.% Bi-ZSM-5 (Si/Al_2 = 250) catalyst is prepared and its activity, as well as, band gaps are compared with that of 3 wt.% Bi-ZSM-5 (Si/Al_2 = 27.5). Small change in the band gap and very low activity observed on Bi-ZSM-5 with Si/Al_2 = 250 (Fig. 10) indicates that presence of acid sites in zeolite is necessary for

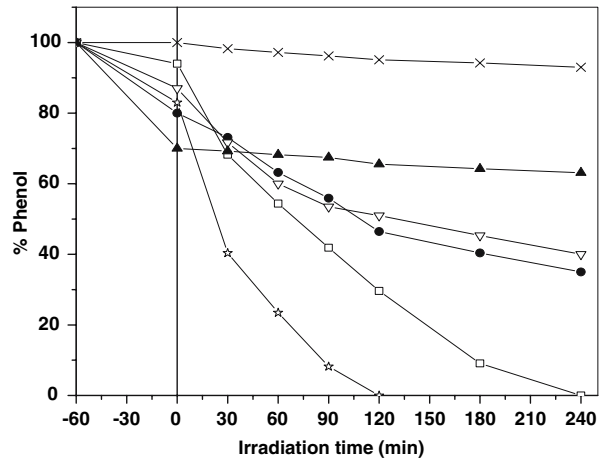

Fig. 8 (×) Photolysis and photocatalytic degradation of phenol (10^{-4} M) over (▲) HZSM-5, Bi-ZSM-5, and (□) Bi_2O_3: (●) 1 wt.% Bi_2O_3, (☆) 3 wt.% Bi_2O_3, and (▽) 5 wt.% Bi_2O_3

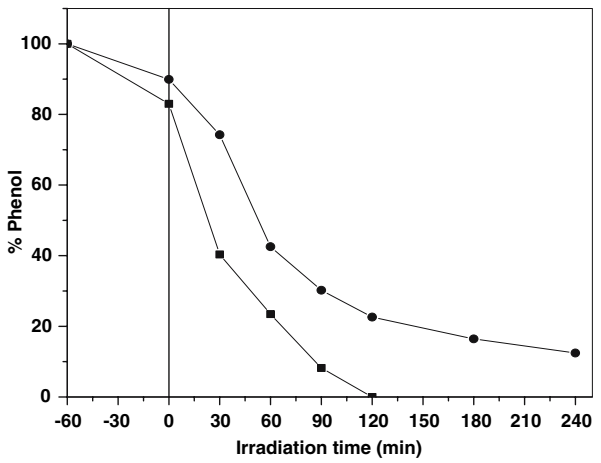

Fig. 10 Degradation of phenol over: (■) Bi-ZSM-5 (3 wt.% Bi_2O_3, Si/Al_2 = 27.5) and (●) Bi-ZSM-5 (3 wt.% Bi_2O_3, Si/Al_2 = 250)

Bi to interact. The photocatalytic activity of Bi_2O_3 dispersed on HZSM-5 by SSD (Fig. 9) is relatively low and the degradation is slow. Though the dispersed Bi_2O_3 particles do show increased band gaps or energy, the band gaps are not comparable with that of Bi-ZSM-5.

These observations confirm the following aspects:

(1) The band gaps arising either through interaction or dispersion of bismuth oxide should be high enough to minimize the electron–hole recombination.
(2) The zeolite should have sufficient Al content to establish linkages with photoactive species.
(3) The zeolite should also be left with some free acid sites to absorb the pollutant molecules and also to act as electron acceptors.
(4) The available amount of photocatalyst and acid sites should be such that the arising synergism results in the best photocatalyst.
(5) The preformed bismuth oxide used may have no interaction with the support and the particles are of usually bigger size leading to decreased band gap resulting in faster *electron–hole* recombination: *a major* disadvantage of the photocatalysts.
(6) Bi_2O_3 in interaction with the HZSM-5 with increased band gap is showing enhanced photoactivity due to the reduced electron–hole recombination.

A plausible photocatalytic mechanism showing difference in the activity with respect to number of hydroxyl radicals produced from the electrons–hole pairs generated by the change in the band gap energy of the catalysts is depicted in Scheme 1.

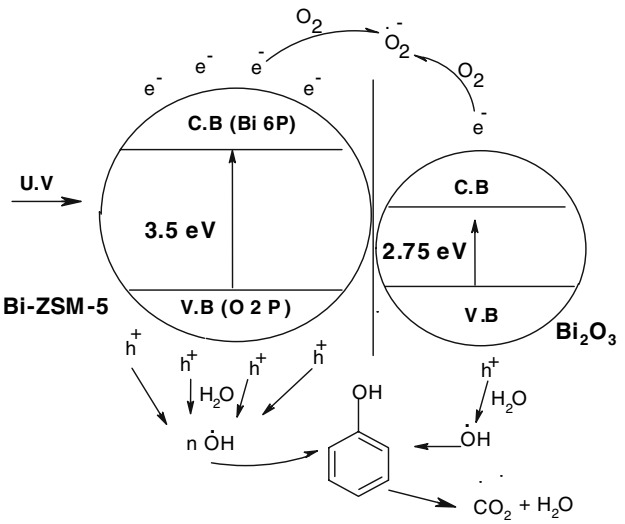

Scheme 1 Band gap vs. photocatalytic activity of the bismuth photocatalysts in the degradation of phenolic wastes

4 Conclusion

Bi-ZSM-5 prepared by simple impregnation method showed the enhanced photocatalytic activity (compared to bare Bi_2O_3) through the increased band gap of bismuth oxide, wherein bismuth oxide particles are isolated and in interaction with the support. The adsorption properties of the support and the increased band gap of interacted bismuth resulted in the enhanced activity of Bi-ZSM-5 catalysts in the photodegradation of phenol.

References

1. Robertson PKJ (1996) J Cleaner Prod 4:203
2. Hoffman MR, Martin ST, Choi W, Bahnemann DW (1995) Chem Rev 95:69
3. Pirkanniemi K, Sillanpaa M (2002) Chemosphere 48:1047
4. Carp O, Huisman CL, Reller A (2004) Prog Solid State Chem 32:33
5. Mills A, Hunte SL (1997) J Photochem Photobiol A 101:1
6. Bhatkhande DS, Pangarkar VG, Beenacker AA (2001) J Chem Technol Biotechnol 77:102
7. Herrmann JM (1999) Catal Today 53:115
8. Ranjit KT, Willner I, Bossman SH, Braun AM (2001) J Catal 204:305
9. Shankar MV, Cheralathan KK, Arabindoo B, Palinichamy M, Murugesan V (2004) J Mol Catal A 223:195
10. Anpo M (2004) Bull Chem Soc Jpn 77:1427
11. Takeuchi M, Kimura T, Hiduka M, Rakhmawath D, Anpo M (2007) J Catal 246:235
12. Noorjahan M, Durga Kumari V, Subrahmanyam M, Boule P (2004) Appl Catal B 47:209
13. Durga Kumari V, Subrahmanyam M, Subbarao KV, Ratnamala A, Noorjahan M, Tanaka K (2002) Appl Catal A 234:155
14. Li W (2006) Mater Chem Phys 99:174
15. Zhang L, Wang W, Yang J, Chen Z, Zhang W, Zhou L, Liu S (2006) Appl Catal A 308:105
16. Leontie L, Caraman M, Delibas M, Rusu GI (2001) Mater Res Bull 36:1629
17. Leonite L, Caraman M, Alexe M, Harnagea C (2002) Surf Sci 480:507
18. Xiaohong W, Wei Q, Weidong H (2006) J Mol Catal A 263:167
19. Weidong H, Wei Q, Xiahong W, Xianbo D, Long C, Zhaohua J (2007) Thin Solid Films 515:5362
20. Zuhang KL, Liu CM, Huang Q, Zheng C, Wang W (2006) Appl Catal B 68:125
21. Lin X, Huang T, Huang F, Wangac W, Shia J (2007) J Mater Chem 17:2145
22. Drache M, Roussel P, Wignacourt JP (2007) Chem Rev 107:80
23. Shuk P, Wiemhofer HD, Guth U, Gopel W, Greenblatt M (1996) Solid State Ionics 89:179
24. Tan PL, Au CT, Lai SY (2007) Appl Catal A 324:36
25. Yuan Q, Hagen A, Roessner F (2006) Appl Catal A 303:81
26. Dumitiu D, Barjega R, Frunza L, Macovei D, Hu T, Xie Y, Parvulescu VI, Kaliaguine S (2003) J Catal 219:337
27. Shido T, Otika G, Asakura K, Iwasawa Y (2000) J Phys Chem B 104:12263